Supporting Information

Bimodal Mesoporous Titanium Nitride/Carbon Microfibers as Efficient and Stable Electrocatalysts for Li-O$_2$ Batteries

Jihee Park,[†] Young-Si Jun,*[† ‡] Woo-ram Lee,[†] Jeffrey A. Gerbec,[‡] Kimberly A. See, [†§‡] and Galen D. Stucky*[†§‡]

[†]Department of Chemistry and Biochemistry, University of California, Santa Barbara, CA 93106 USA, [§]Materials Department, University of California, Santa Barbara, CA 93106 USA, [‡] Mitsubishi Chemical-Center for Advanced Materials (MC-CAM), University of California, Santa Barbara, CA 93106 USA,   Mitsubishi Chemical USA, Chesapeake, VA 23320 USA

*E-mail: youngsi.jun@gmail.com, stucky@chem.ucsb.edu

EXPERIMENTAL DETAILS

Synthesis of bmp-TiN/C: Melamine (3.96 mmol) dissolved in 20 ml DMSO was mixed with equimolar TCA (3.96 mmol) dissolved in 10 ml DMSO. MTCA microfibers were obtained by adding 30 ml H$_2$O into the above solution. The mixture was filtered, washed with H$_2$O and dried at 90 °C. Before the infiltration of titanium precursor, the MTCA crystal was pre-heated at 350 °C. The preheated MTCA (0.3 g) was infiltrated with a titanium tetrachloride (0.1 g) solution in ethanol (6 g) and dried at room temperature for overnight. bmp-TiN/C as a black powder was finally obtained after heating at 800 °C for 3 h with a heating rate of 5 °C min^{-1} under nitrogen.

Characterization: SEM/TEM images were taken with Hitachi S4800 and JEOL FB-2100F (HR) at an acceleration voltage of 200 kV, respectively. Powder X-ray diffraction was carried out in reflection mode (Cu Kα radiation) on a Scintag X2 θ-θ diffractometer. Nitrogen sorption analysis was conducted at -196 °C using a Micromeritics ASAP 2020. FT-IR spectra were collected on a JASCO FT-IR 470 plus with the average of 12 scans with a resolution of 4 cm^{-1} from 4000 cm^{-1} to 600 cm^{-1}. XPS spectra were provided by ESCALAB250.

Electrochemical analysis

Air cathode preparation: bmp-TiN/C, conductive carbon black (Super P, Timcal), and polyvinylidene fluoride (PVDF) polymer binder (2:6:2) were stirred in cyclopentanone for 3 hr. The dispersions of the reference Super P, Pt/C (ETEK, 20wt% Pt), and bmp-TiN/C alone were prepared with PVDF (8:2). The resulting dispersion was cast on carbon paper (AvCarb P75T) as a gas diffusion layer (GDL) and dried at 120 °C for overnight in order to remove the residual cyclopentanone or moisture. The carbon loading amount per GDL is 0.9 mg±0.2 mg.

Electrolyte Preparation: TEGDME (Sigma) was distilled over a packed bed column and dried for several days over freshly activated molecular sieves (type 4Å). Battery grade lithium triflate (Sigma, CF$_3$SO$_3$Li, 99.995%) was used without further purification. A CF$_3$SO$_3$Li solution in TEGDME (molar ratio of 1:4) was prepared as an electrolyte at least one day before use.

Electrochemical Measurement: Potentiodynamic cycling with galvanostatic acceleration (PCGA) was conducted in CR2032 coin cells comprised of a polished lithium metal anode (10 mm), an electrolyte (0.4 ml) impregnated two-sheets of glass fiber separator (GFC, Whatman, 19 mm), and an air cathode (19 mm). The cells were assembled in an Ar-filled glove box and operated with a VMP 3 Biologic Instrument. The positive can was machine-drilled to make 21 holes (1 mm diameter and 2 mm distance) for oxygen flow. Linear sweep voltammetry under Ar atmosphere (Figure S7) indicates the anodic decomposition of cell components, i.e. polymer binder, electrolyte, and electrode, above 4.6 V. The upper cut off potential is, therefore, set at 4.5 V for the electrochemical analysis. The lower one is set at 2.0 V well below the equilibrium potential of oxygen reduction. PCGA analysis was performed by setting stepwise potential scans of 5 mV with a minimum current limit of 3 µA and a maximum single potential step duration of 1h, within a discharge/charge capacity of 1000 mAh/g. The cell was first inserted into the coin cell holder and then placed in a beaker-type oxygen chamber in an Ar-filled glove box. The oxygen chamber was purged with pure oxygen for more than 5 h before analysis. Galvanostatic cycling with potential limitation (GCPL) operation was conducted in the same cell configuration, while oxygen is continuously flowed into the beaker chamber via Schlenk line and vented through an oil bubbler in order to maintain the oxygen pressure slightly higher than 1 atm.

Potential window: Accumulation of an insulating discharge product, Li_2O_2, or side reaction products such as LiCOOH, Li_2CO_3, and $LiRCO_3$ passivates the surface of cathode and also induces pore blocking of a gas diffusion layer (GDL). This inhibits the electrical contact among catalyst, electrolyte, and di-oxygen molecules and increases polarization resistance during charge procedure after deep discharge to 2.0 V vs. Li/Li^+. Upper limit of the operation potential was set at 4.5 V vs. Li/Li^+ above which the organic cell components such as electrolyte, polymer binder, conductive carbon, and carbon paper, are decomposed at above 4.5 V vs. Li/Li^+. The cells could not completely recover the discharge capacity in the potential ranges. We, therefore, set the discharge potential to be moderate as 2.4 V vs. Li/Li^+ in order to avoid complete passivation of GDL.
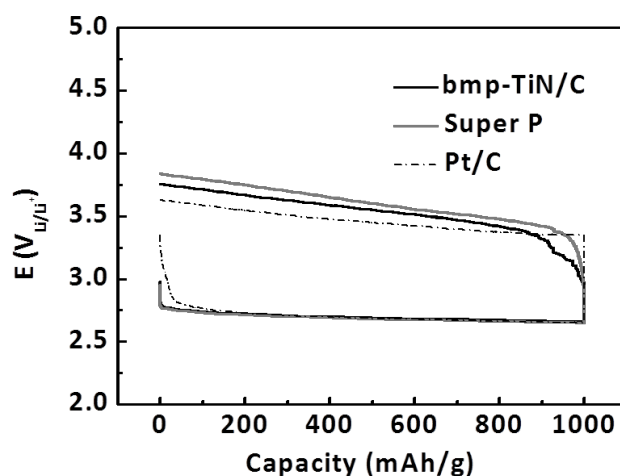

Figure S1 PCGA profiles of bmp-TiN/C, Super P, and Pt/C at a charge capacity of 1,000 mAh/g
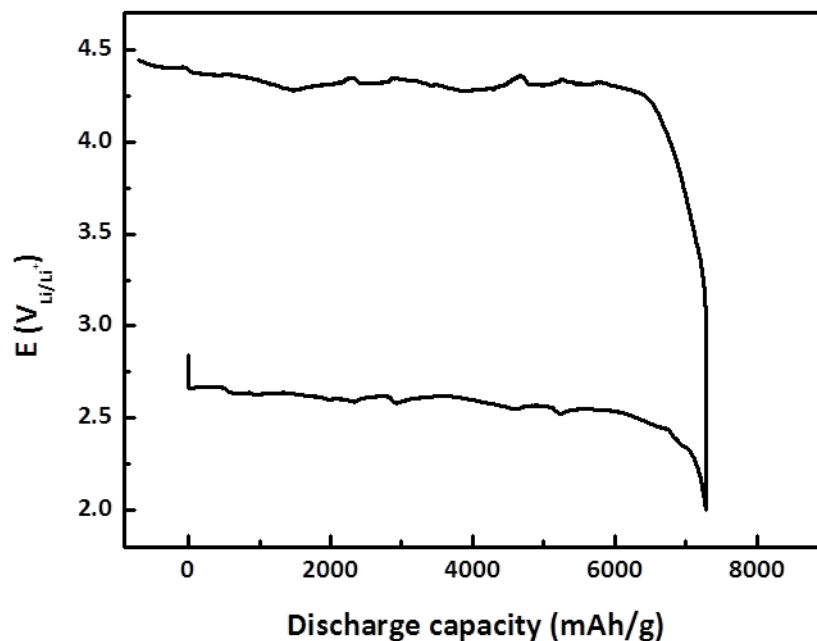
Super P·

Figure S2 Discharge-charge profile of bmp-TiN/C alone at 100 mA/g $_{bmp-TiN/C}$ in the potential ranges between 2.0~4.5V. bmp-TiN/C alone enables the full discharge-charge cycle with a capacity of 7,285 mAh/g $_{bmp-TiN/C.}$

TEGDME (tetraethylene glycol dimethyl ether) is known to be more stable than carbonate solvent-based electrolytes against oxygen radicals.[1] Especially, TEGDME and Li^+ form solvent separated ion pairs (SSIP) at 1 to 4~5 molar ratio of $LiCF_3SO_3$ to TEGDME.[2] The SSIP facilitates the mass transfer of dissolved di-oxygen molecules and inhibits the side reactions between oxygen radical and free TEGDME molecules during discharge procedure, improving the cycling performance of $Li-O_2$ batteries.

When $LiCF_3SO_3$/TEGDME (1:4 molar ratio) is utilized as an electrolyte in the present work, Li_2O_2 is a major product after discharge in the presence of Super P or TiN/C catalysts, indicating that the discharge capacity generated by the $Li-O_2$ cells mainly resulted from the formation of Li_2O_2. This, however, does not mean that TEGDME based electrolyte is completely free from the oxidative decomposition during the reversible formation and dissociation of Li_2O_2. Although the anodic decomposition of the organic cell components including $LiCF_3SO_3$/TEGDME was not observed in the presence of TiN/C-Super P mixture catalyst at the potential ranges lower than 4.6 V vs. Li/Li^+ (Figure S7), the interplay among Li_2O_2 (highly oxidative), TEGDME, and carbon consisted of Super P, PVDF, carbon paper, or bmp-TiN/C induces the side reactions forming CO_2, $Li2CO_3$, $LiRCO_3$, and $LiCOOH$ and renders the charge procedure inefficient by insulating the cathode and thus increasing polarization resistance. The formation of side products is further accelerated under potential bias more than 3.5 V vs. Li/Li^+.[3] This is why the charge profile shows a plateau slowly increasing up to 4.5 V vs. Li/Li^+. Abrupt potential increase in the charge profile can be observed in the potential ranges higher than 4.5 V vs. Li/Li^+ as a result of the

complete electrolytic or electrocatalytic dissociation of Li_2O_2 or Li_2CO_3. The anodic decomposition of TEGDME will also occur in the potential range, making it difficult to distinguish the two events.
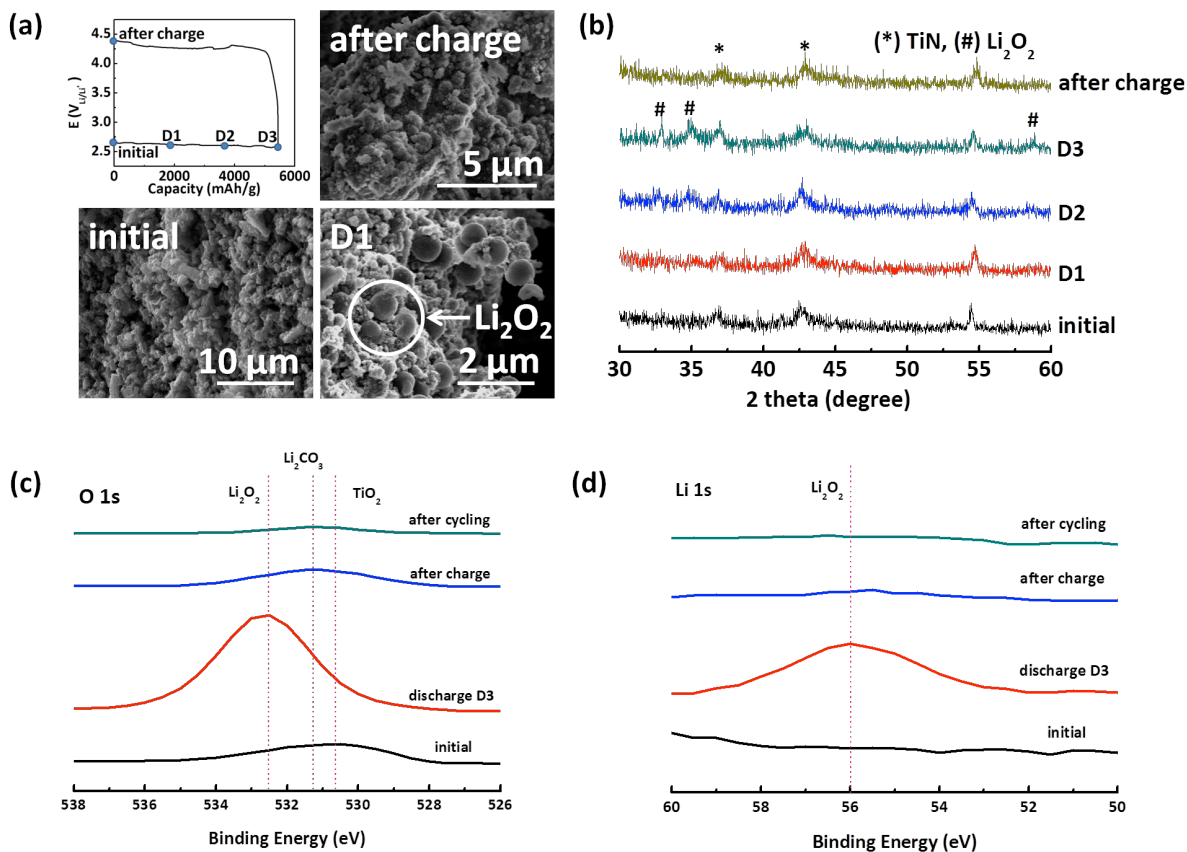

Figure S3 (a) SEM images, (b) XRD patterns, and (c) O 1s and (d) Li 1s XPS spectra of bmp-TiN/C alone electrodes at a current density of 100 mA/g $_{bmp-TiN/C}$. D1: 25%, D2:50%, D3:80% discharge depth based on the full discharge capacity of 7,285 mAh/g $_{bmp-TiN/C}$ of Figure S2.
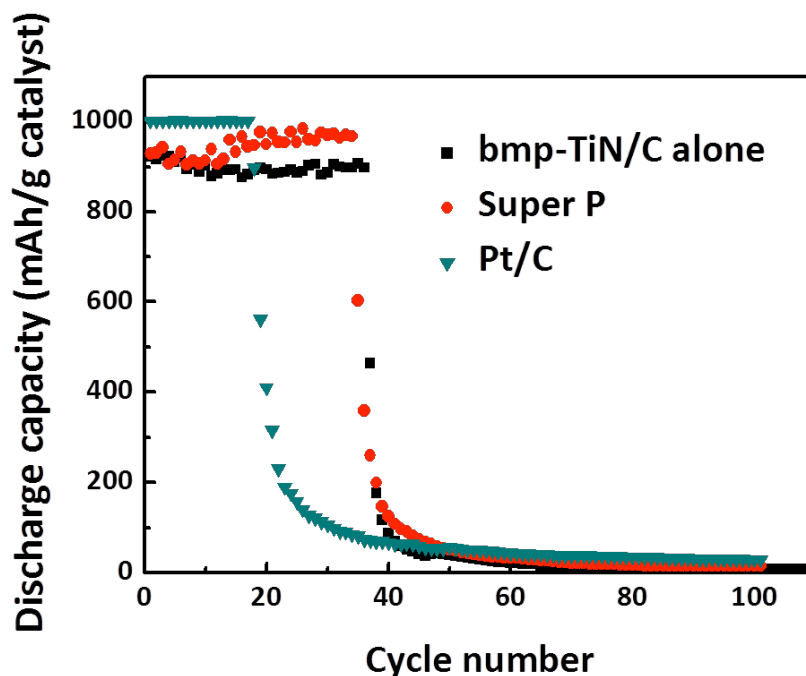
Figure S4 Cycling performance of bmp-TiN/C alone, Super P, bmp-TiN/C mixed with Super P and Pt/C electrodes at a current density of 200 mA/g catalyst and a discharge capacity of 1000 mAh/g catalyst with a potential limit of 2.0 ~4.5 V.
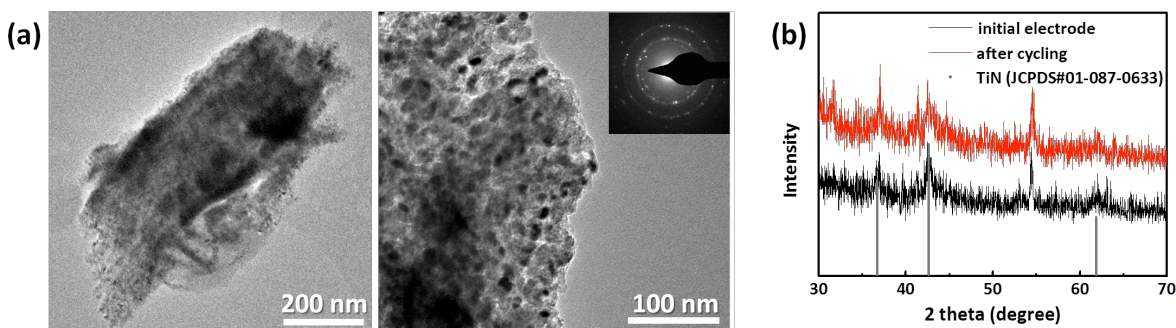

Figure S5 (a) TEM images of bmp-TiN/C and (b) X-ray diffraction patterns after cycling under a current density of 200 mA/g with a capacity limit of 1000 mAh/g. The inset of TEM image shows the corresponding selected area electron diffraction (SAED) pattern, which was intact compared to that of the as-prepared bmp-TiN/C shown in Figure 2. Carbothermal reduction of preformed TiO_2 using g-CN under nitrogen or NH_3 atmosphere induces the insertion of C or O in small amounts into the crystal structure of TiN,[4,5] acting as a protection barrier to further oxidation. The oxidation stability of TiN in bmp-TiN/C during discharge and charge procedures was proved by XRD, SEM, and TEM in Figure 2, S3, and S5 and briefly discussed in page 3 column 1 and 2 due to the page limitation. As shown in XRD patterns, TEM and SEM images, and SAED patterns in Figure 2, S3, and S5, crystal structure of TiN nanoparticle and macroscopic morphology of bmp-TiN/C were intact before and after cycling. We believe that these are enough to prove stability of the electrocatalyst.
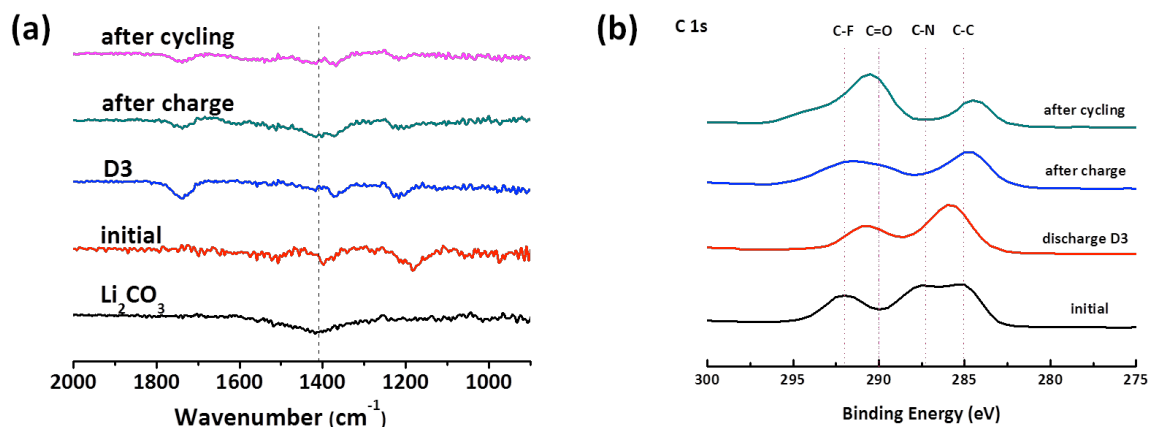
Figure S6 (a) FT-IR spectra and (b) C 1s XPS spectra of bmp-TiN/C alone cathode at the stage of discharge (D3), then subsequent charge as indicated in figure S3 and after cycling. The peaks at 879, 1186, and 1406 cm^{-1} arise from PVDF. The carbonate formation is more pronounced in the electrode after charge than that after cycling probably due to the anodic decomposition of carbonates during charging procedure to 4.5V.
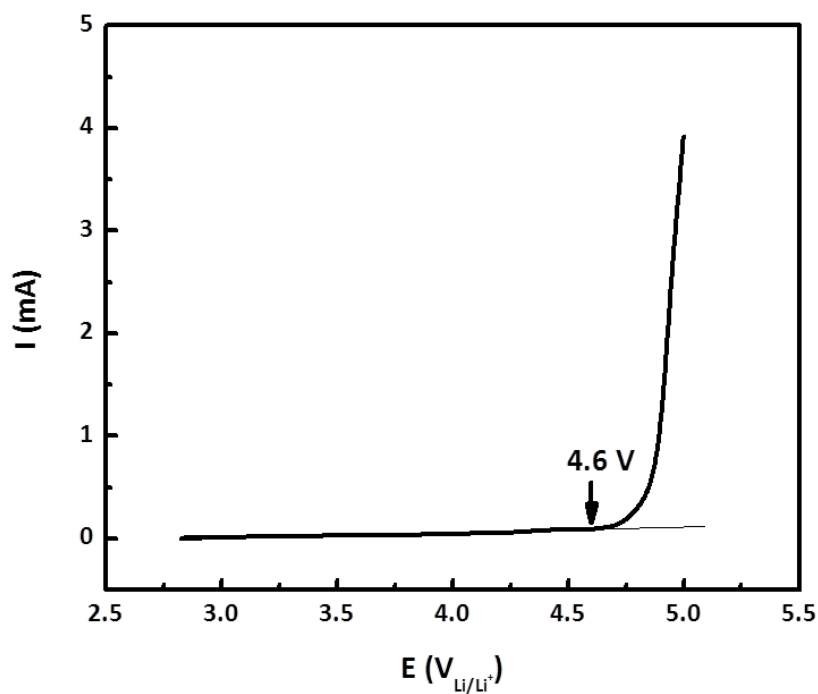

Figure S7 Linear sweep voltammogram of two-electrode cells with a lithium metal and a carbon paper loaded with bmp-TiN/C mixed with Super P under an O$_2$ atmosphere. Scan rate: 0.1 mV/s.

References

(1) Jung, H.-G.; Hassoun, J.; Park, J.-B.; Sun, Y.-K.; Scrosati, B. *Nature Chemistry* 2012, *4*.

(2) Fujun, L.; Tao, Z.; Yamada, Y.; Yamada, A.; Haoshen, Z. *Advanced Energy Materials* 2013, *3*, 532.

(3) Thotiyl, M. M. O.; Freunberger, S. A.; Peng, Z.; Bruce, P. G. *Journal of the American Chemical Society* 2013, *135*, 494.

(4) Jun, Y. -S.; Hong, W. H.; Antonietti, M.; Thomas, A. *Advanced Materials* 2009, *21*, 4270.

(5) Ohnishi, R.; Katayama, M.; Cha, D.; Takanabe, K.; Kubota, J.; Domen, K. *Journal of the Electrochemical Society* 2013, *160,* F501.